

CPPM Machine: A Synchronous Permanent Magnet Machine with Field Weakening

Juan A. Tapia, Thomas A. Lipo, *Fellow, IEEE*

Dept. of Electrical and Computer Engineering
University of Wisconsin-Madison
1415 Engineering Dr
Madison WI 53706-1651 USA
Tel:(608) 265-0727 Fax (608) 262-5559

Franco Leonardi

Vehicle Electronic Systems Department
Ford Research Laboratories
Dearborn MI. USA
Tel/fax 313-390 6923

Abstract

Due to its particular configuration, the Consequent Pole Permanent Magnet (CPPM) machine allows one to easily control the airgap flux in a wide range so that the power capability of the machine is increased over a wide speed range. Two components of the flux, one -almost constant- coming from the permanent magnet located on the rotor surface of the machine, and the other -variable- coming from a field winding located in the middle of the stator, converge in the airgap characterizing the level of excitation of the machine. The field winding -when a variable DC current is injected- provides an adaptable level of excitation in both positive and negative directions respect to the PM magnetization. In this manner, control of the airgap flux can be obtained with a reduced amount of field MMF. A prototype using this configuration has been built and experimental results show that with 10% of the phase MMF it is possible to vary the flux in a range over +/-40%.

Key Words : PM machine, Field Weakening, Design PM machines

1. Introduction

Permanent magnet machines, in traction applications, are usually designed to provide constant torque up to a base speed, and constant power from the base speed up to the maximum speed defined for the mechanical constraint [1]. To perform this constant power operation field weakening has to be considered in order to respect the current and voltage limitations of the converter that transform the fixed voltage-frequency utility power into variables ones. To reduce the excessive excitation generated for the PM at high speed, several techniques have been proposed in the literature. Negative current in the *d*-axis produces a demagnetizing effect, which reduces the flux in the airgap. This approach is used for vector control technique to drive the machine along the maximum torque per ampere trajectory [2,3]. However, this method implies conduction losses [4] and additional risk of demagnetization of the polar pieces [5]. In fact, due to the low permeability of the modern permanent magnet, near to the air value, the current necessary to reach an adequate level of control is high and the heat

created for this process elevates the PM temperature, which go in detriment of their characteristic. Changing the magnetic circuit of the machine represents a different method to handle the high-speed over excitation. In [6], a two-rotor segment machine combines part PM and reluctance structures. Rearranging the stator coil so that the back emf is regulated according to the speed is also possible [7].

The CPPM machine combines the fixed excitation of the rare earth permanent magnet with the variable flux given by a field winding. In that way, airgap flux can be controlled in a wide range with minimum conduction losses and without demagnetization risk for the PM pieces. This feature allows to extend the speed range of the machine, operate at unity power factor and obtain full utilization of the inverter's VA capacity to transfer active power to the output [8].

This paper compares the field weakening operation of a synchronous PM machine, under maximum torque per ampere (MTA) technique and excitation control to operate at unity power factor. Also, a prototype of the CPPM machine is presented and its airgap control capabilities are explored. A 3KW prototype 8-pole, 3-phase, using this configuration has been built and experimental results show that using this configuration, less than 10% of the AC winding mmf is necessary to vary the airgap flux in a +/- 40% range.

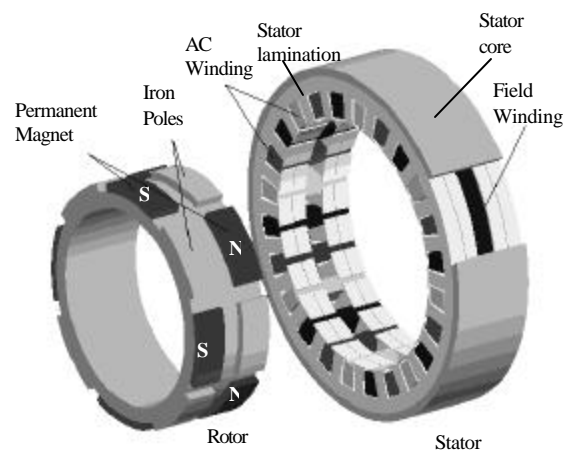


Fig. 1. 8-poles CPPM machine structure.

2. Description of the CPPM

Fig. 1 shows the structure of the CPPM machine. The machine consists of a two-rotor section with partial surface-mounted permanent magnets structure, which are radially and consequently magnetized. One stator with partial solid yoke to diminish the inter-lamination airgap and a conventional three-phase winding. Additionally, a circumferential field winding in the middle of stator provides a variable excitation.

The radial magnetization of the permanent magnets creates an almost constant flux, which circulates from one pole to the next one across the stator and rotor yoke, teeth, and PM pieces. This portion of the flux is determined mainly for the PM's geometry and the reluctance of its path. In this case, the airgap and magnet reluctances are the most important values. On the other hand, injecting DC current into the field winding generates a flux which goes from the one iron pole to another through the stator and rotor yoke, with a path entirely composed of this material, except for the main airgaps. Due to the comparative low reluctance of this path, the DC current flowing through the field winding can easily control this flux. The combination of these two fluxes produces a variable level of excitation in the machine according to the magnitude and direction of the DC current. Fig 2, outlines the per pole flux path under different DC field currents.

- For no field current, the flux in the machine is only due to the PM, and because the magnetization is consecutive, the trajectory of the flux from one section to the next crosses the stator yoke in the oblique direction, Fig. 2a.
- When the flux generated by the field winding flows in the direction showing in Fig. 2b, where it is added to the PM, the flux closes its path in the same magnetic pole. In other words, in the airgap, flux coming from the PM and the iron pole, crosses the airgap in opposite directions. As a result, the total flux per pole decreases as the field flux increases. Flux crosses the stator yoke axially.
- If the field current is reversed, the field flux changes its direction. The total airgap flux is the summation of both components. Therefore, as the field current increases, the flux per pole increases. Flux closes its path crossing the stator yoke azimuthally. Fig. 2c.

The Consequent Pole Permanent Magnet machine presents several advantages in comparison with the regular PM machine such as:

- Wide range of airgap flux control to reduce or increase its value. This is accomplished with a low requirement for field ampere-turns.

- This particular configuration permits one to control the level of excitation of the machine without any demagnetisation risk for the permanent magnet parts.
- Airgap flux control allows one to increase and improve the power capability at low, medium and high-speed ranges of the drive-motor configuration

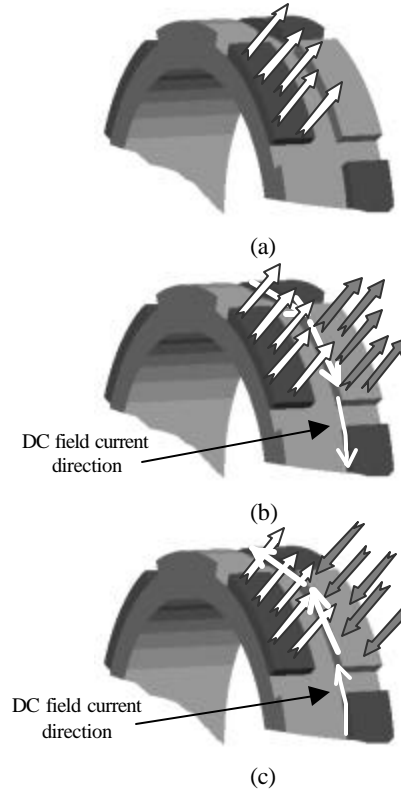


Figure 2. Airgap flux composition with field current excitation.

3. Power Capability Analysis

Based on the phasor diagram of the salient pole synchronous machine, Fig.3, the following expression can be derived

$$E \sin d = X_q I \cos(d - f) \cos d + X_d I \sin(d - f) \sin d \quad (1)$$

$$E \cos d = V - X_q I \cos(d - f) \sin d + X_d I \sin(d - f) \cos d \quad (2)$$

Combining equation (1) and (2), an expression for the torque angle can be found

$$\tan d = \frac{X_q I \cos(d - f) \cos d + X_d I \sin(d - f) \sin d}{V - X_q I \cos(d - f) \sin d + X_d I \sin(d - f) \cos d} \quad (3)$$

Solutions to these expressions provide the information to determine the correct excitation to perform unity power factor control. Conversely, MTA control calculates the proportion of I_d and I_q in which the stator

current is divided, such that the maximum torque available is obtained subject to the inverter constraints. It was demonstrated in [9] that the optimum machine parameter values to extend the speed range of the drive occur when the back-emf at rated speed is numerically equal to the direct axis reactance in pu.

$$E_o = X_d \quad (\text{in per unit}) \quad (4)$$

This theoretical relation assures that with a rated current at a high speed the output power approximates to 1 pu.

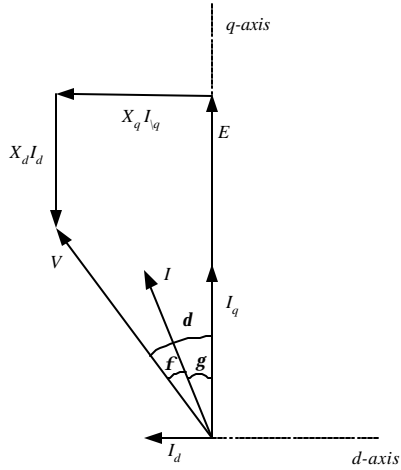


Figure 3. Phasor diagram for salient pole machine

In the following subsections comparative analysis were done base on the performance of the PM drive under MTA and unity power factor control.

3.1 Comparison with Ideal MTA Control. ($E_o = X_d$)

With MTA control below the rated speed, each component of the phasor diagram of Fig. 3, increases linearly with the frequency, each component of the stator current is constant, and the torque is constant at the optimum value. When the speed goes over the rated value the back-emf increase linearly (saturation for this analysis is not considered) and field-weakening control takes place to accomplish voltage restriction. As a result, *d-axis* current increases its value to counterbalance the excessive excitation, and *q-axis* current diminishes to increase the torque angle.

Controlling the excitation, the power factor can be settled at unity over all the speed operation. To compensate the linear variation of $X_d I_d$ voltage, the back-emf has to increase according to eq. (1,2,3). In that way, current and voltage are in-phase all the time and the total VA of the inverter is utilized as active power to the output. At high speed both voltages change with the same ratio, like in the MTA case.

Fig. 4 shows the output power for both control technique. Due to the low level of magnetization provided for the PM in the MTA case, some of the VA has to be provided for the inverter to the machine.

Therefore the power factor at a low speed is less than unity. The dotted line represents this situation. When the excitation is provided by an internal mechanism like a field winding, the inverter no longer has to supply the magnetization; therefore the complete capacity of the inverter can be utilized to produce real power. (Solid line).

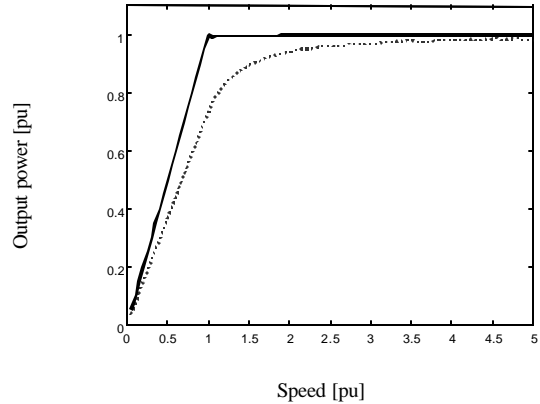


Figure 4. Power Capability curve, ideal MTA case (dotted line) and unity power factor control (solid line)

Fig 5 shows the evolution of each phasor diagram's component of Fig. 3. For maximum torque per ampere control, the linear variation of the back-emf is expected. At a high speed it became parallel to the *d-axis* voltage. When airgap control is considered, the variation of the *d-axis* voltage is followed for the excitation so that the power factor is unity and in similar manner at MTA control, both voltages are parallel at high speed.

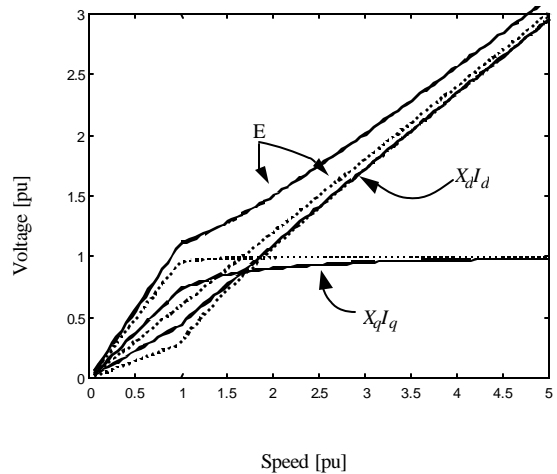


Figure 5. Control performance comparison. Solid line: unity power factor. Dotted line: MTA control ($E_o = 0.6$ pu). Machine parameters: $X_{ds} = 0.6$ pu, $X_{ds} = 1.1$ pu.

For an ideal parameter condition, eq. (4), a machine with field-weakening capability exhibits better performance than a regular PM machine under MTA control. Airgap flux control allows to maximize the

available VA of the inverter improving the drive power capability in all speed ranges. Resistive effects can also be overcome incrementing the excitation at a very low speed.

3.2 Comparison with non-ideal MTA Control. ($E_o \neq X_d$)

When condition (4) is not accomplished, the speed range under maximum torque per ampere control is reduced dramatically. In fact, the unbalance between the variation of the open circuit voltage, E , and d -axis voltage drop as speed increase over the rated value provokes an unstable condition. Due to the unequal ratio of change of both voltages, their difference augments in accordance with the speed. That difference produces a reduction of the q -axis current to compensate quadrature voltage drop. Fig 6 (dotted lines). With that, current rotates counter clock-wise and power factor decreases. As speed increases the volt-amperes of the inverter are transformed in reactive power and torque capability is reduced.

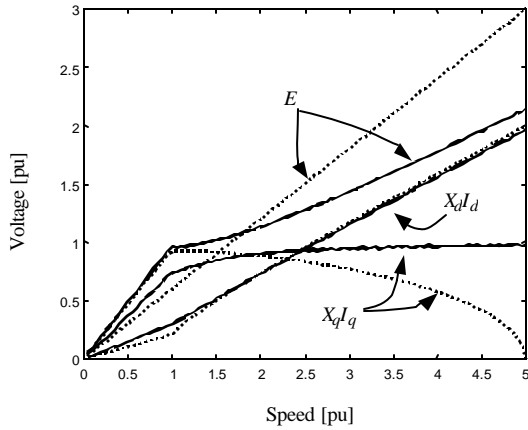


Figure.6. Open circuit voltage and reactive voltage drop for (a) MTA control ($E_o=0.6$ pu), and (b) Unity power factor control. Machine parameters: $X_{ds}=0.4$ pu, $X_{qs}=1.1$ pu.

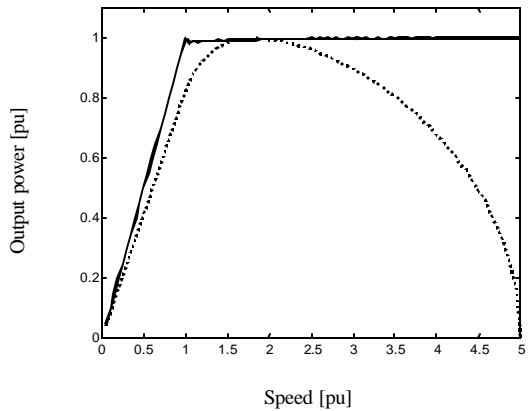


Figure. 7. Power Capability curve, non-ideal MTA case (dotted line) and unity power facto control (solid line)

With excitation control the difference between the open voltage circuit and d -axis reactance voltage drop is compensated. For any reasonable value of X_b the airgap flux can be adjusted so that the excitation can follow the reactance voltage drop. In that way, condition (4) can always be achieved, in addition to the unity power factor. Fig 7 (solid line).

In a non-ideal case, where the parameters of the machine do not match (4), the power capability of the machine under MTA control is reduced drastically due to the unequal variations of the back-emf and d -axis voltage drop. However, for a machine with airgap flux control capability, as described in the previous section, excitation can be manipulated so that condition (4) is always achieved even though the parameters are not ideal, and the optimal operation is obtained over all speed range.

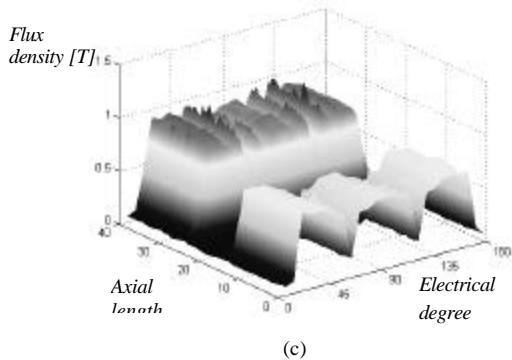
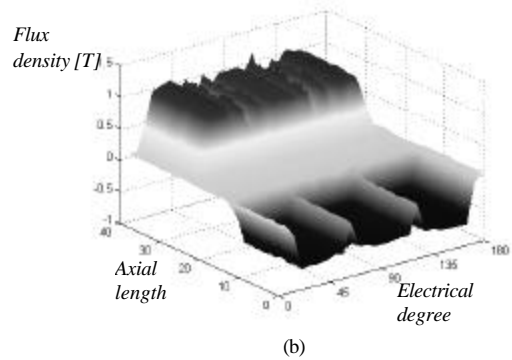
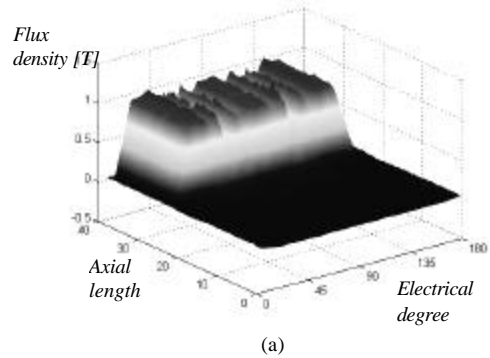


Fig. 8. Airgap flux distribution for one pole and different field AT. a) No field current, b) -500 AT, c) 500 AT

4. Finite Element Analysis

To find out the flux distribution of the CPPM machine, a 3D finite element analysis is carried out. Due to the special configuration, 1/4 of the machine is analysed, including 2poles. Fig. 8 shows three conditions for the airgap flux where the field current is varied from -500 up to 500 ampere-turns.

Due to the comparative low reluctance of the iron respect to the PM, the action of the field current is mostly located over the iron pole. For no-field current, the airgap flux is due only by the PMs, Fig 8a. Increasing the field current in both directions, demagnetizing and magnetizing effects are obtained as is shown in Fig 8 b and c. Little variation of the flux associated to the PM between extreme conditions is observed, due to the saturation produced by the variable flux.

5. Experimental Results

To verify the field control capability of the CPPM machine a 3KW 8-poles 3-phases prototype was built. Fig 9 shows the stator, rotor and housing of the machine. Fig. 10 presents the no-load output voltage under three field current conditions. The rms value of the voltage is varied over a +/- 30 % which reflects the change of the airgap flux.

The magnetic design plays an important role in the performance on the field control capacity. Due to the 3D flux distribution of the flux, airgaps associated to the interlamination and junction between lamination and yokes reduce the ability to control the airgap flux. In fact, according with FEA for the same range of field current a wide variation was expected. However, actual data obtained indicates that improvement in the magnetic circuit is necessary in order to achieve better control.

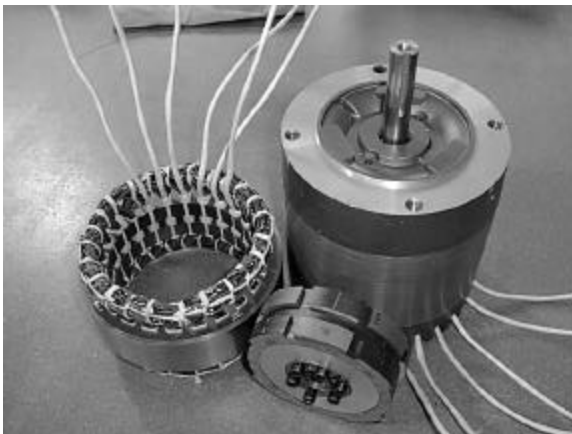


Figure 9. CPPM machine prototype

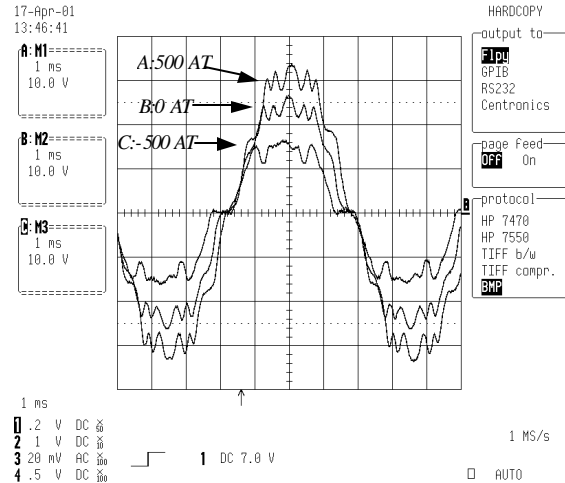


Figure 10. Oscillograph of the CPPM machine's output voltage.
A:23.46 Vrms B:18.13 Vrms, C:11.52 Vrms

6. Conclusions

This paper describes the operating principles; power capability analysis; finite element analysis and the prototype performance of the Consequent Pole Permanent Magnet machine. This magnetic configuration allows to control the flux in the airgap without affecting the magnetization characteristics of the permanent magnets pieces.

Appropriate excitation level allows to perform unity power factor control and to extend the speed range of the drive over a wide range of velocity. Optimum utilization of the inverter VA under this condition is obtained and improvement of the power capability at low and high speed is also achieved.

Experimental results establish that the airgap is controlled over a range of +/- 30 % of the non-field current condition. Optimisation of the magnetic circuit has to be considered in order to improve control range and flux level in the machine

References

- [1] G. R. Slemon, "Achieving a Constant Power Speed Range for OM Drives ", **IEEE Transaction on Industry Application**, Vol.31 No.2, March/April 1995, pp 368-372
- [2] M. Zordan, P. Vas, M. Rashed S. Bolognani, M. Zigliotto. "Field Weakening in high-performance PMSM Drives: a comparative analysis." **Conference Record of the 2000 IEEE Industry Applications Conference**, Vol. 3 , pp 1718 -1724.
- [3] T. M. Jahns, "Motion Control with Permanent-Magnet AC Machines." **Proceedings of the IEEE**, Volume: 82 Issue: 8 , Aug. 1994, pp. 1241 -1252
- [4] F. Leonardi, P. J. McCleer, T. Lipo, "The DSPM: An AC Permanent Magnet Traction Motor with True Filed Weakening" **2nd International**

- Conference on "All Electric Combat Vehicle"**, Detroit MI, June 1997.
- [5] Y. Sozer D.A. Torrey, "Adaptive Flux Weakening Control of Permanent Magnet Synchronous Motor." **IEEE Industrial Application Society Conference Meeting**. St Louis 1998.
- [6] B.J Chalmers, R. Akmese, L.Musaba. "Design and Field-Weakening performance of Permanent /Reluctance Motor with Two-Part rotor." IEE Proceedings - Electric Power Applications. Vol 145, No. 2 March 1998, pp 133-139.
- [7] F. Liang J.M. Miller, X. Xu, "A Vehicle Electric Power Generation System with Improved Output Power ." **IEEE Transaction on Industry Application**, Vol.35 No.6, Nov/Dec 1999
- [8] R. Krishnan, "Electric Motor Drives: Modelling, Analysis, and Control" (book), Prentice Hall, Inc. 2001.
- [9] R.F.Schiferl, T.A. Lipo, "Power Capability of Salient Pole Permanent Magnet Synchronous Motors in Variable Speed Drive Applications" **IEEE Transaction on Industry Application**, Vol.26 No.1, January/February 1990, pp 115-123